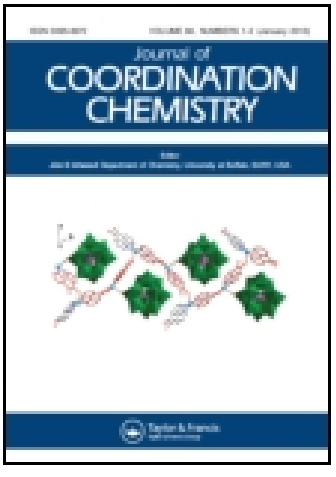


Journal of Coordination Chemistry
Publication details, including instructions for authors and subscription information:
http://www.tandfonline.com/loi/gcoo20

# Synthesis, characterization, and biological activities of macrocyclic polyamine complexes

Q.R. Cheng[a], D. You[a], H. Hu[a], H. Zhou[a] & Z.Q. Pan[a]
[a] Key Laboratory for Green Chemical Process of Ministry of Education, Wuhan Institute of Technology, Wuhan, PR China
Accepted author version posted online: 24 Mar 2014.Published online: 14 Apr 2014.



To cite this article: Q.R. Cheng, D. You, H. Hu, H. Zhou & Z.Q. Pan (2014) Synthesis, characterization, and biological activities of macrocyclic polyamine complexes, Journal of Coordination Chemistry, 67:5, 910-920, DOI: 10.1080/00958972.2014.905685

To link to this article: http://dx.doi.org/10.1080/00958972.2014.905685

*Journal of Coordination Chemistry*, 2014
Vol. 67, No. 5, 910–920, http://dx.doi.org/10.1080/00958972.2014.905685





# Synthesis, characterization, and biological activities of macrocyclic polyamine complexes

Q.R. CHENG, D. YOU, H. HU, H. ZHOU and Z.Q. PAN*

Key Laboratory for Green Chemical Process of Ministry of Education, Wuhan Institute of Technology, Wuhan, PR China

(*Received 8 October 2013; accepted 26 February 2014*)

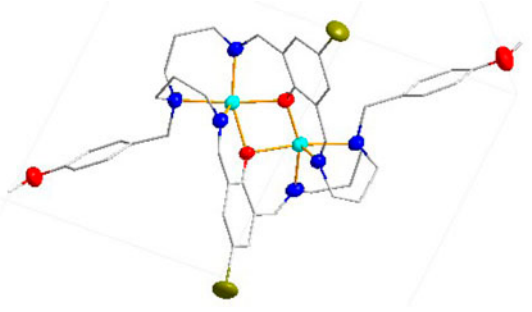

Two new dinuclear macrocyclic polyamine complexes have been synthesized and characterized by infrared spectra, elemental analysis, ES-MS spectrum, and X-ray single crystal diffraction. The interactions of the complexes with CT-DNA have been measured by spectroscopy, viscosity, electrochemical measurements, and the agarose gel electrophoresis.

Two new dinuclear macrocyclic complexes, $[Ni_2L^1(OAc)]\cdot ClO_4$ (**1**) and $[Co_2L^2(OAc)]\cdot 1.5(ClO_4)\cdot 0.5Na\cdot 2(CH_3OH)$ (**2**) (where $H_2L^1$ and $H_2L^2$ are the condensation products of N,N-bis(3-aminopropyl)-4-methoxybenzylamine with 2,6-diformyl-4-brominephenol and 2,6-diformyl-4-methylphenol in the presence of metal ions, respectively) have been synthesized and characterized by infrared spectra, elemental analysis, electrospray mass spectra, and X-ray single crystal diffraction. The interactions of the complexes with CT-DNA have been measured by UV-absorption titrations and fluorescence quenching experiments.

*Keywords*: Polyamine; Macrocyclic dinuclear complex; Binding mode; DNA cleavage

## 1. Introduction

Polyamines have value in the study of biological activities and new materials [1]. Hettich and Schneider synthesized a series of polyamine cobalt complexes by modifying cyclen and

*Corresponding author. Email: zhiqpan@163.com

trpn ligands [2]. Simulation enzyme research on Schiff base macrocyclic complexes has made progress, and Martell found that this kind of complex can simulate activity of tyrosine [3]. Deoxyribonucleic acid (DNA) is the carrier of biological genetic information and plays an important role in the process of life. Research has shown that there are two potential targets in medicine, DNA and tyrosine kinase, in cancer treatment drug design [4]. Therefore, an important way for chemotherapy drugs research is to design new DNA-insertion agents. The development of artificial metallonucleases as cellular regulators of DNA is of interest in therapeutic and biochemical technology [5–7]. The search for artificial metallonucleases that can cleave DNA hydrolytically is a particular challenge because of the long intrinsic half-life for hydrolysis of DNA at pH 7 and 25 °C [8, 9]. Kandaswamy and co-workers have synthesized a series of binuclear copper(II) complexes of macrocyclic polyamine ligands with two phenol groups, and they found that this kind of complex binds to DNA in an intercalative mode [10]. In contrast, nickel(II) complexes of macrocyclic polyamines with two phenol groups have received much less attention. In fact, nickel(II) complexes with macrocyclic ligands were also found to have potential DNA cleavage reactivity [11]. In numerous nuclease simulations, complexes formed by macrocyclic polyamines in coordination have good nucleic acid activity [12]. Researchers mainly determine the combination model of complexes and DNA by methods such as ultraviolet, fluorescence, circular dichroism, viscosity, and electrochemical experiments [13].

Macrocyclic polyamine complexes are widely used in many chemical fields and occupy important positions in nucleic acid cutting and drug design of DNA targets because of their flexible structures. This makes study of these complexes important. In order to establish correlations between the binding structure and the reactivity toward DNA cleavage, we designed two new dinuclear macrocyclic complexes and studied the DNA cleavage activity of the complexes by spectroscopic analysis. The structures of the complexes are shown in scheme 1.

## 2. Experimental

### 2.1. *Materials*

All chemicals were purchased from commercial sources and used as received. Solvents were dried according to standard procedures and distilled prior to use.

2,6-Diformyl-4-bromophenol was synthesized according to a procedure reported previously [14]. 4-Methoxybenzylamine and nickel(II) perchlorate hexahydrate were purchased from Alfa Aesar. Tris(hydroxylmethyl)-amino-methane (Tris), bromophenol blue, ethidium bromide (EB), agarose gel, and plasmid pBR322 DNA were purchased from Toyobo Co.

### 2.2. *Synthesis of the complexes*

**2.2.1. N,N-bis(2-cyanoethyl)-4-methoxybenzylamine (cmba).** Cmba was synthesized by an improved literature method [15]. To a solution of 4-methoxybenzylamine (13.7 g, 0.1 M) in distilled water (100 mL), acrylonitrile (16.0 g, 0.3 M) was added dropwise at 5 °C, then the resulting mixture was refluxed for 90 h. After returning to room temperature, the mixture was extracted with dichloromethane, and the organic layer was washed with brine and dried with anhydrous sodium sulfate. After filtration, the solvent was removed to give the

product as a yellow oil. Yield: 23.5 g (97%). The oil was used for the following reaction without purification.

**2.2.2. N,N-bis(3-aminopropyl)-4-methoxybenzylamine (amba).** A mixture of cmba (23.5 g, 0.097 M) in methanol (200 mL) and active Raney-Ni (10.0 g) was vigorously stirred, and a solution of $NaBH_4$ (11 g, 0.291 M) in 8 M/L NaOH (70 mL) was added at such a rate as to maintain the temperature at 60 °C. After the addition was complete, the reaction mixture was stirred at room temperature overnight. The Raney-Ni catalyst was then removed by filtration, and the solvent was removed under reduced pressure. The crude amba was extracted with dichloromethane and dried with anhydrous sodium sulfate. After filtration, the solvent was distilled off to obtain the crude product as a colorless oil. Yield: 21.5 g (88%). Amba·3HCl was prepared by acidifying amba with an HCl–EtOH solution, and white precipitate was obtained. The precipitate was washed with EtOH several times and dried in vacuo. The pure product was obtained as its trihydrochloride by recrystallization from a minimum of water and ethanol [16]. Yield: 26.5 g (86%). Anal. Calcd for $C_{14}H_{28}ON_3Cl_3$: C, 46.6; H, 7.8; N, 11.7. Found: C, 45.8; H, 7.3; N, 12.1. IR (KBr, $cm^{-1}$): 3051, 2913 (C–H), 3359 (N–H), 1247, 1032 (C–O). $^1H$ NMR ($D_2O$, d/ppm): 7.13 (d, 2H, 2ArH), 6.83 (d, 2H, 2ArH), 3.67 (s, 3H, –O–$CH_3$), 3.38 (s, 2H, Ar–$CH_2$), 2.45 (t, 4H, 2$CH_2$–$NH_2$), 2.28 (t, 4H, 2N–$CH_2$), 1.51 (m, 4H, 2–$CH_2$–).

**2.2.3. $[Ni_2L^1(OAc)]\cdot ClO_4$ (1).** Amba·3HCl (0.18 g, 0.5 mM) was dissolved in $H_2O$ (10 mL) and neutralized with NaOH (0.06 g, 1.5 mM), and the solution was added to a mixture of 2,6-diformyl-4-bromophenol (0.082 g, 0.5 mM) and $Ni(OAc)_2\cdot 4H_2O$ (0.124 g, 0.5 mM) in ethanol (10 mL). The mixture was stirred overnight, and then $NaClO_4\cdot H_2O$ (0.07 g, 0.5 mM) in ethanol (10 mL) was added. After stirring for another 6 h, a yellow precipitate was collected. Green single crystals suitable for X-ray structure analysis were obtained by evaporation of an acetonitrile solution of the complex. Yield: 0.13 g (50%). Anal. Calcd for $C_{46}H_{53}O_{10}N_6Ni_2Br_2Cl$: C, 47.5; H, 4.6; N, 7.2. Found: C, 46.8; H, 5.0; N, 7.7. IR (KBr, $cm^{-1}$): 3051, 2913 (C–H), 1642(C=N), 1081, 624 ($ClO_4^{-1}$), 1247, 1032 (C–O).

**2.2.4. $[Co_2L^2(OAc)]\cdot 1.5(ClO_4)\cdot 0.5Na\cdot 2(CH_3OH)$ (2).** Amba·3HCl (0.18 g, 0.5 mM) was dissolved in $H_2O$ (10 mL) and neutralized with NaOH (0.06 g, 1.5 mM). The organic phase was extracted with chloroform (4 × 15 mL), and the combined organic phase was dried over anhydrous sodium sulfate. The solvent was removed under reduced pressure to obtain grease. The grease was dissolved in absolute methanol (10 mL) and added to a mixture of 2,6-diformyl-4-bromophenol (0.082 g, 0.5 mM) and $Pb(OAc)_2\cdot 4H_2O$ (0.198 g, 0.5 mM) in methanol (10 mL). The mixture was stirred overnight, and then $Co(OAc)_2\cdot 4H_2O$ in methanol (10 mL) was added. After stirring for 8 h, a brown precipitate was obtained. One more equivalent of $Co(OAc)_2\cdot 4H_2O$ (0.113 g, 0.5 mM) in methanol (10 mL) was added, and stirring was continued for another 8 h when precipitation was complete. After filtration via vacuum and drying, a brown precipitate was collected. Brown single crystals suitable for X-ray structure analysis were obtained by evaporation of an acetonitrile solution of the complex. Yield: 0.15 g (52%). Anal. Calcd for $C_{50}H_{67}O_{14}N_6Co_2Cl_{1.5}Na_{0.5}$: C, 51.8; H, 5.8; N, 7.2.

Found: C, 51.7; H, 5.9; N, 7.3. IR (KBr, $cm^{-1}$): 3051, 2913 (C–H), 1642(C=N), 1081, 624 ($ClO_4^{-1}$), 1247, 1032 (C–O).

### 2.3. *Physical measurements*

IR spectra were measured using KBr disks on a Vector 22 FTIR spectrophotometer. $^1H$ NMR spectra were recorded on a Varian Mercury VX-300 spectrometer at 30 °C in $D_2O$ with TMS as the internal reference. Elemental analyses were obtained on a Perkin-Elmer 240 analyzer. Electrospray mass spectra (ES-MS) were determined on a Finnigan LCQ ES-MS mass spectrograph using methanol as the mobile phase with an approximate concentration of 1.0 mM $dm^{-3}$. Absorption spectra of 190–700 nm were recorded on a Shimadzu UV-2450 spectrophotometer. Fluorescence spectra were recorded on a Jasco FP-6500 spectrophotometer.

### 2.4. *Structure determination*

Diffraction intensity data were collected on a SMART CCD area-detector diffractometer at 291 K using graphite monochromated Mo Kα radiation ($\lambda = 0.71073$ Å). Data reduction and cell refinement were performed with SMART and SAINT [17]. The structure was solved by direct methods (Bruker SHELXTL) and refined on $F^2$ by full-matrix least squares (Bruker SHELXTL) using all unique data [18]. All non-hydrogen atoms were refined anisotropically and hydrogens were refined on calculated positions using a riding mode. The crystal data are listed in table 1. Selected bond lengths and angles are provided in table 2.

Table 1. Crystal data and details of the structure for **1** and **2**.

| | | |
|---|---|---|
| Empirical formula | $C_{46}H_{53}ClN_6Br_2Ni_2O_{10}$ | $C_{50}H_{67}Cl_{1.5}N_6Co_2O_{14}Na_{0.5}$ |
| Formula weight | 1162.63 | 1158.63 |
| Crystal system | Monoclinic | Monoclinic |
| Space group | *P21/n* | *P21/c* |
| *a*, *b*, *c* [Å] | 16.505(2), 17.220(3), 18.368(3) | 18.003(1), 20.113(1), 15.585(1) |
| *α*, *β*, *γ* [°] | 90, 97.088, 90 | 90.00, 110.925, 90.00 |
| Volume | 5180.6(13) | 5271.3(8) |
| *Z* | 4 | 4 |
| $D_{Calcd}$ | 1.491 | 1.460 |
| *μ* (Mo Kα) [/nm] | 2.380 | 0.780 |
| *F* (0 0 0) | 2376 | 2424 |
| Crystal size ($mm^3$) | 0.20 × 0.10 × 0.10 | 0.16 × 0.12 × 0.10 |
| Temp. (K) | 298(2) | 173(2) |
| Mo Kα radiation (Å) | 0.71073 | 0.71073 |
| *θ* Range (°) | 1.96–25.5 | 2.03–25.10 |
| Index ranges | $-19 \le h \le 17$, $-20 \le k \le 18$, $-22 \le l \le 22$ | $-21 \le h \le 21$, $-24 \le k \le 24$, $-18 \le l \le 16$ |
| Nref, Npar | 9613, 607 | 9363, 704 |
| Tot., uniq. data *R*(int) | 31,057, 9613, 0.0584 | 31,174, 9363, 0.0720 |
| Observed data [$I > 2.0\sigma(I)$] | 5754 | 6778 |
| *R*, $wR_2$, *S* | 0.0692, 0.1998, 1.103 | 0.0737, 0.1932, 1.106 |
| Min. and Max. Resd. Dens. [e $Å^{-3}$] | −0.669, 0.945 | −0.924, 0.880 |

Table 2. Selected bond distances (Å) and angles (°) for **1** and **2**.

| **1** | | | | **2** | | | |
|---|---|---|---|---|---|---|---|
| Bonds | Length (Å) | Bonds | Length (Å) | Bonds | Length (Å) | Bonds | Length (Å) |
| N4–Ni1 | 2.066(5) | N1–Ni2 | 2.074(5) | Co1–O5 | 2.062(3) | Co2–O6 | 2.077(3) |
| N6–Ni1 | 2.098(5) | N3–Ni2 | 2.085(5) | Co1–O2 | 2.064(3) | Co2–O4 | 2.081(3) |
| N5–Ni1 | 2.214(5) | N2–Ni2 | 2.193(5) | Co1–O4 | 2.102(4) | Co2–O2 | 2.111(3) |
| Ni1–O1 | 2.050(4) | Ni2–O5 | 2.039(5) | Co1–N6 | 2.098(4) | Co2–N3 | 2.100(3) |
| Ni1–O6 | 2.054(5) | Ni2–O2 | 2.054(4) | Co1–N2 | 2.101(4) | Co2–N5 | 2.123(4) |
| Ni1–O2 | 2.089(4) | Ni2–O1 | 2.076(4) | Co1–N1 | 2.232(5) | Co2–N4 | 2.242(4) |
| Bond angles | Values (°) | Bond angles | Values (°) | Bond angles | Values (°) | Bond angles | Values (°) |
| O1–Ni1–O6 | 85.90(17) | N6–Ni1–N5 | 81.8(2) | N1–Ni2–N2 | 91.2(2) | N6–Co1–N1 | 89.47(17) |
| O1–Ni1–O2 | 77.79(17) | O5–Ni2–O2 | 85.66(17) | N3–Ni2–N2 | 83.3(2) | N2–Co1–N1 | 81.77(17) |
| O6–Ni1–O2 | 92.55(17) | O5–Ni2–O1 | 90.92(17) | O5–Co1–O4 | 91.41(14) | O6–Co2–O4 | 86.75(13) |
| O1–Ni1–N4 | 159.4(2) | O2–Ni2–O1 | 78.01(16) | O2–Co1–O4 | 77.78(13) | O6–Co2–O2 | 92.98(14) |
| O6–Ni1–N4 | 87.3(2) | O5–Ni2–N1 | 86.1(2) | O5–Co1–N6 | 87.32(16) | O4–Co2–O2 | 77.23(13) |
| O1–Ni1–N6 | 84.52(18) | O2–Ni2–N1 | 159.4(2) | O2–Co1–N6 | 159.55(16) | O6–Co2–N3 | 89.05(15) |
| O6–Ni1–N6 | 164.87(19) | O5–Ni2–N3 | 166.8(2) | O5–Co1–N2 | 163.95(17) | O4–Co2–N3 | 158.95(15) |
| O2–Ni1–N6 | 96.83(19) | O2–Ni2–N3 | 85.83(18) | O2–Co1–N2 | 85.39(15) | O6–Co2–N5 | 161.78(15) |
| O1–Ni1–N5 | 109.70(18) | O1–Ni2–N3 | 97.18(19) | O5–Co1–N1 | 86.93(16) | O4–Co2–N5 | 84.83(15) |
| O6–Ni1–N5 | 90.43(19) | O5–Ni2–N2 | 89.6(2) | O2–Co1–N1 | 110.11(15) | O2–Co2–N5 | 100.86(15) |
| O2–Ni1–N5 | 172.14(17) | O2–Ni2–N2 | 107.54(18) | O4–Co1–N1 | 171.85(14) | O6–Co2–N4 | 86.43(15) |
| N4–Ni1–O2 | 83.1(2) | O1–Ni2–N2 | 174.45(18) | N6–Co1–O4 | 82.48(16) | O4–Co2–N4 | 111.49(15) |
| N4–Ni1–N6 | 105.6(2) | N1–Ni2–O1 | 83.30(19) | N2–Co1–O4 | 101.32(16) | O2–Co2–N4 | 171.19(14) |
| N4–Ni1–N5 | 89.8(2) | N1–Ni2–N3 | 105.2(2) | N6–Co1–N2 | 103.86(17) | N3–Co2–O2 | 82.40(14) |



### 2.5. *DNA-binding experiments*

CT-DNA (20 mg) was dissolved in Tris–HCl buffer (100 mL, 50 mM Tris–HCl, 50 mM NaCl, pH 7.2) and kept at 4 °C for less than four days. The absorption ratio $A_{260}/A_{280}$ was within the range of 1.8–2.0. The DNA concentration was determined via absorption spectroscopy using the molar absorption coefficient of 6600 $M^{-1}$ $cm^{-1}$ (260 nm) for CT-DNA [19].

The complex was dissolved in DMF at $5.09 \times 10^{-5}$ M. UV absorption titrations were performed by keeping the concentration of the complex fixed while varying the DNA concentration. Complex-DNA solutions were allowed to incubate for 30 min at room temperature before measurements were made. Absorption spectra were recorded using cuvettes of 1 cm path length at room temperature. The intrinsic binding constant $K_b$ was calculated according to equation (1) [20]:

$$[\mathrm{DNA}]/E_{ap} = [\mathrm{DNA}]/E + 1/(K_b E) \quad (1)$$

$$E_{ap} = \varepsilon_a - \varepsilon_f, E = \varepsilon_b - \varepsilon_f$$

in which $\varepsilon_a$, $\varepsilon_f$, and $\varepsilon_b$ are the molar extinction coefficients of solutions containing both complex and DNA, free complex, and the complex bound to DNA, respectively.

Fluorescence quenching experiments were performed by adding a solution of the complex (1.5 μL) to EB-bound CT-DNA solution (1.5 μL) at different concentrations (12.5–200 μM). All experiments were carried out using cuvettes of 1-cm path length at room temperature. Samples were excited at 520 nm and emission was recorded at 450–750 nm.

## 3. Results and discussion

### 3.1. *Synthesis and characterization*

In the IR spectrum of **1**, the sharp C=N stretching vibration bands corresponding to imine groups of the macrocyclic framework are observed at 1642 $cm^{-1}$, indicating that a macrocyclic complex has been synthesized. In addition, strong bands at 1081 and 624 $cm^{-1}$ can be ascribed to $ClO_4^-$.

The ES-MS spectrum of **1** in methanol solution (Supplementary data S1, see online supplemental material at http://dx.doi.org/10.1080/00958972.2014.905685) is dominated by a peak at *m/z* 1063.42, corresponding to $[Ni_2(OAc)L^1]^+$ ($C_{46}H_{53}O_6N_6Ni_2Br_2$, Calcd 1063.12). Theoretical and experimental isotope distribution of the main peaks of **1** is shown in the inset, revealing good agreement between observed and calculated data. The other peaks in the ES-MS of the nickel(II) complex are not discussed, due to their low abundance (<5%). The ES-MS spectrum shows that $[Ni_2(OAc)L^1]^+$ is stable in methanol solution.

In addition, **2** was synthesized using $Pb(OAc)_2$ as template and metal ion exchange. The similarity of the relative vibration bands of IR in **2** is in agreement with the comparability of its crystal structure.

The ES-MS spectrum of **2** in methanol solution (Supplementary data S2) is dominated by a peak at *m/z* 933.67, corresponding to $[Co_2(OAc)L^2]^+$ ($C_{48}H_{59}O_6N_6Co_2$, Calcd 933.87). Theoretical and experimental isotope distribution of the main peaks of **2** is shown in the inset, revealing good agreement between observed and calculated data. The other peaks in the ES-MS of the Co(II) complex are not discussed, due to their low abundance (<5%). The ES-MS spectrum shows that $[Co_2(OAc)L^2]^+$ is stable in methanol.

### 3.2. *Crystal structures*

**3.2.1. $[Ni_2L^1(OAc)]ClO_4$ (1).** A perspective view of $[Ni_2L^1(OAc)]ClO_4$ is given in figure 1. The nickel complex is composed of a $[Ni_2(OAc)L^1]^+$ cation and a perchlorate. The two Ni ions reside in the $N_3O_2$ sites of the macrocycle $[L^1]^{2-}$. Deviation of Ni(1) and Ni(2) from the mean plane, formed by O1, O2, N5, and N6 and by O1, O2, N2, and N3, are 0.1711(8) and

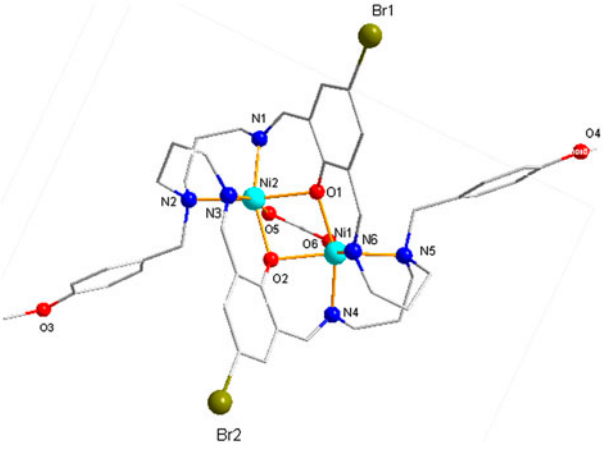


Figure 1. Crystal structure of **1**; hydrogens have been omitted for clarity (ellipsoids are drawn at 30% probability).

0.1710(8) Å, respectively. The dihedral angle between the planes is 27.9°. The angle between the two benzene rings in each complex is 59.58°. The basal bond distances around Ni(1) are 2.050–2.214 Å. The apical bond distances are Ni(1)–N(6) = 2.098(5) Å and Ni(1)–O(6) = 2.054(5) Å, with the bond angle O(6)–Ni(1)–N(6) = 164.87(19)°. The bond distances around Ni(2) are 2.054–2.193 Å. The apical bond distances are Ni(2)–N(3) = 2.085(5) Å, Ni(2)–O(5) = 2.039(5) Å, with the bond angle O(5)–Ni(2)–N(3) = 166.8(2)°. The nickel–nickel separation bridged by the two phenolic oxygens is 3.148 Å with Ni–O–Ni angles of 99.43° and 98.93°.

**3.2.2. $[Co_2L^2(OAc)]\cdot 1.5(ClO_4)\cdot 0.5Na\cdot 2(CH_3OH)$ (2).** A perspective view of $[Co_2L^2(OAc)]\cdot 1.5(ClO_4)\cdot 0.5Na\cdot 2(CH_3OH)$ (**2**) is given in figure 2. The Co(II) complex is composed of a $[Co_2(OAc)L^2]^+$, a perchlorate, and two methanols. There is a position occupied by a perchlorate or $Na^+$, the probability of 50% each one. The two Co ions reside in the $N_3O_2$ sites of the macrocycle $[L^2]^{2-}$. Deviation of Co(1) and Co(2) from the mean plane, formed by O2, O4, N1, and N6, and O2, O4, N3, and N4, are 0.1891(7) Å and 0.1946 Å, respectively. The dihedral angle between the planes is 30.39°. The angle between the two benzene rings in each complex is 64.38°. The basal bond distances around Co(1) are 2.062–2.232 Å. The apical bond distances are Co(1)–N(2) = 2.101(4) Å, Co(1)–O(5) = 2.062(3) Å, with the bond angle O(5)–Co(1)–N(2) = 163.95(17)°. The bond distances around Co(2) are 2.077–2.242 Å. The apical bond distances are Co(2)–N(5) = 2.123 Å, Co(2)–O(6) = 2.077 Å, with the bond angle N(5)–Co(2)–O(6) = 161.78°. The cobalt–cobalt separation bridged by the two phenolic oxygens is 3.175 Å with Co–O–Co angles of 98.73° and 99.00°.

### 3.3. *Spectroscopic analysis of DNA-binding activity*

Electronic absorption spectroscopy is one of the most useful methods for DNA-binding studies of metal complexes. Intercalative binding of a complex to DNA generally results in hypochromism along with a redshift of the band [21].

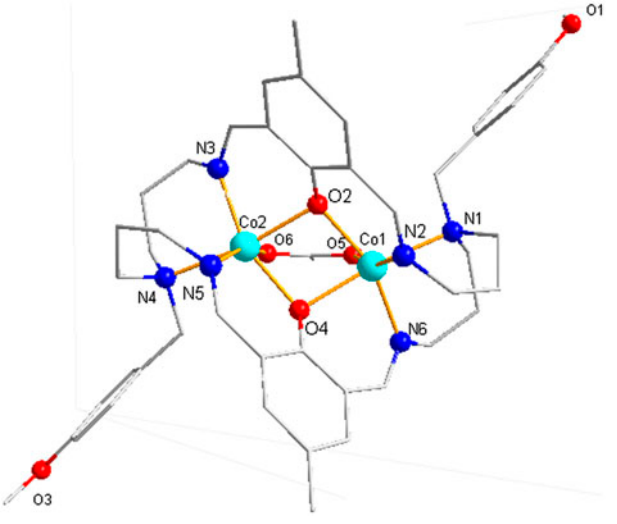


Figure 2. Crystal structure of **2**; hydrogens have been omitted for clarity (ellipsoids are drawn at 30% probability).

The absorption spectra of the nickel(II) complex in the absence and presence of CT-DNA at different concentrations (0–150 μM) are given in figure 3.

The spectrum of the Ni(II) complex shows a very strong absorption at 393 nm, which is attributed to a metal-to-ligand charge transfer (MLCT) [22, 23]. The band shows a bathochromic shift of 19 nm and hypochromism of 15.8% after adding DNA. The value of $K_b$ was obtained from the ratio of slope to the intercept from the plot of [DNA]/($\varepsilon_a - \varepsilon_f$) *versus* [DNA] as $2.04 \times 10^4\ M^{-1}$.

Absorption spectra of the Co(II) complex in the absence and presence of CT-DNA at different concentrations (0–150 μM) are given in figure 4.

The spectrum of the Co(II) complex shows a very strong absorption at 391 nm, which is attributed to a MLCT. Different from **1**, hyperchromic effect occurred in **2** absorption spectra. Hyperchromic effect means that the secondary structure of DNA was destroyed by the complexes. The band shows the max bathochromic shift of 34 nm and hyperchromism of 36.6% after adding DNA. The insert mode between complexes and DNA results in a hypochromic effect. Therefore, the binding mode between **2** and DNA is not the insert mode. The $K_b$ value is $1.22 \times 10^5\ M^{-1}$. We deduce that the Co(II) complex binds to DNA with a moderate groove mode.

Compared to other complexes, $K_b$ of **1** is lower than those of the nickel(II) complexes $Ni(HAdr)_2$ ($4.3 \times 10^4$), $[Ni(L)(SCN)_2]$ ($1.07 \times 10^5$), and $[Ni_2L_1(ClO_4)]^+$ ($2.8 \times 10^5$) [24–26] and slightly higher than that of the nickle(II) complex $[Ni(QTS)_2]^+$ ($3.27 \times 10^3$) [27]. $K_b$ of **2** is higher than those of the cobalt(II) complexes $[Co(bmbb)_2](pic)_2$ ($7.95 \times 10^4$) and [Co(DCA)(bipy)($H_2O$)] ($4.02 \times 10^4$) [28, 29].

Mixed solutions of DNA and EB show very strongly enhanced fluorescence emission [30] due to intercalation of EB to DNA. The binding of the complex to DNA can be determined according to the classical Stern–Volmer equation (2):

$$I_0/I = 1 + K[Q] \tag{2}$$

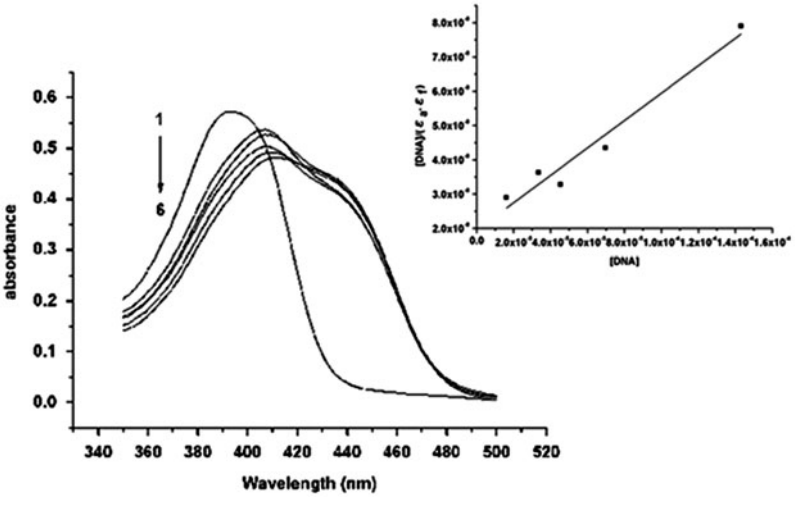


Figure 3. UV–visible spectra of **1** in the presence of increasing amounts of CT-DNA in 50 mM Tris–HCl buffer solution (pH 7.2). [$M_1$] = 50 μM; 2–6: [$M_1$] + [DNA]. [DNA] = 16, 33, 45, 70, 145 μM.

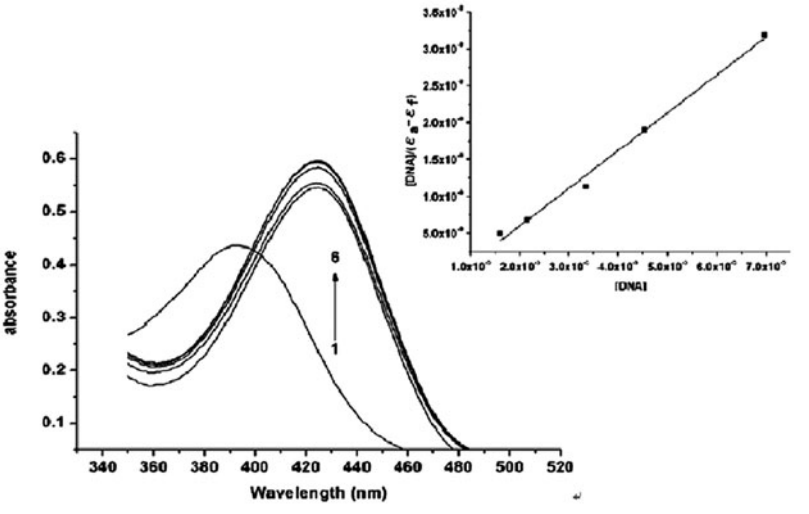


Figure 4. UV–visible spectra of **2** in the presence of increasing amounts of CT-DNA in 50 mM Tris–HCl buffer solution (pH 7.2). $[M_2] = 50\ \mu M$; 2–6: $[M_2]$ + [DNA]. [DNA] = 16, 21.5, 33, 45, 70 μM.

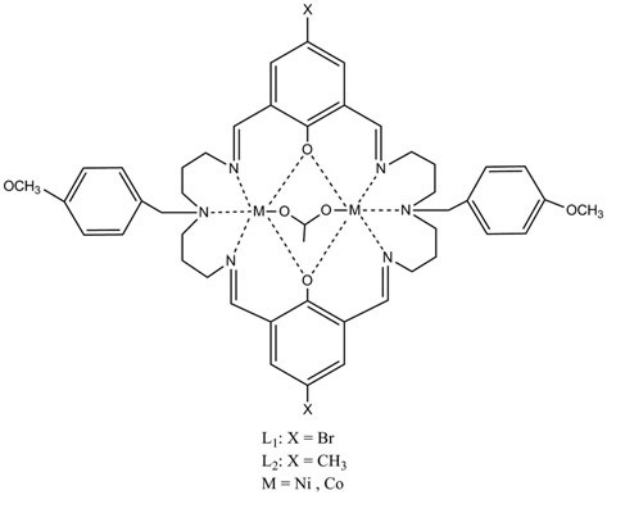


Scheme 1. Chemical structure of the complexes.

in which $I_0$ and $I$ are the fluorescence intensities of EB-DNA in the absence and presence of complex, respectively, K is the linear Stern–Volmer quenching constant, and [Q] is the concentration of the complex [31]. The fluorescence intensity at 605 nm ($\lambda_{ex} = 520$ nm) of EB in the bound form was plotted against the compound concentration.

Emission spectra of EB bound to DNA in the absence and presence of **1** are given in Supplementary data S3. When the Ni(II) complex was added to the EB-DNA system, the emission intensity was reduced. The constant is $2.3 \times 10^3\ M^{-1}$, which is smaller than those of DNA-intercalative complexes, so we deduce that the Ni(II) complex binds to DNA with a moderate intercalative mode.

Similar to **1**, when the Co(II) complex was added to the EB-DNA system, the emission intensity was reduced. The emission spectra of EB bound to DNA in the absence and presence of **2** are given in Supplementary data S4. The constant is $2.12 \times 10^3\ M^{-1}$. From the ultraviolet spectrum variation of **2**, we deduce that **2** binds to DNA with a moderate groove mode.

Compared to other complexes, $K_q$ of **1** is lower than those of the nickel(II) complexes $Ni(HAdr)_2$ ($3.4 \times 10^4$), $[Ni(L)(SCN)_2]$ ($6.9 \times 10^4$), $[Ni_2L_1(ClO_4)]^+$ ($1 \times 10^7$), and $[Ni(L)_2]_4$·EtOH ($3.2 \times 10^5$) [24–26, 32], and $K_q$ of **2** is also lower than those of the cobalt(II) complexes $[Co(bmbb)_2](pic)_2$ ($3.76 \times 10^4$) and $[Co(DCA)(bipy)(H_2O)]$ ($1.08 \times 10^{15}$) [28, 29].

## 4. Conclusion

Two new macrocyclic complexes have been synthesized and structurally characterized. The biological activities of the complexes toward calf thymus DNA were studied by UV absorption and fluorescence spectroscopy. The binding constants of **1** and **2** are $2.04 \times 10^4\ M^{-1}$ and $1.22 \times 10^5\ M^{-1}$, respectively. The linear Stern–Volmer quenching constants calculated from fluorescence experiments for **1** and **2** are $2.3 \times 10^3\ M^{-1}$ and $2.12 \times 10^3\ M^{-1}$, respectively. The results indicate that **1** binds to DNA by a moderate intercalation mode and **2** binds to DNA by a moderate groove mode.

## Supplementary material

Crystallographic data for the structures reported in this article have been deposited at the Cambridge Crystallographic Data Center, CCDC Nos. 963138 and CCDC 963139. Copies of the data can be obtained free of charge on application to CCDC, 12 Union Road, Cambridge CB2 1EZ, UK [Fax: +44 1223 336-033; E-mail: deposit@ccdc.cam.ac.uk].

## Funding

We are thankful for the financial support from the National Nature Science Foundation of China [grant numbers 21301131, 51374158]; the Nature Science Foundation of Hubei Province [grant number 2013CFB313]; the open fund of Engineering Research Center of Nano-Geo Materials of Ministry of Education China University of Geosciences, Wuhan [grant number CUGNGM201311]; and the scientific research fund of Wuhan Institute of Technology [grant number 10122013].

## References

[1] H. Zhou, Z.Q. Pan, H.P. Zhang, J.D. Hu, X.L. Hu. *Transition Met. Chem.*, **31**, 163 (2006).
[2] R. Hettich, H.J. Schneider. *J. Am. Chem. Soc.*, **119**, 5638 (1997).
[3] D.A. Rockcliffe, A.E. Martell. *Inorg. Chem.*, **32**, 3143 (1993).
[4] M.F. Braña, G. Domínguez, B. Sáez, C. Romerdahl, S. Robinson, T. Barlozzari. *Eur. J. Med. Chem.*, **37**, 541 (2002).
[5] Z.F. Chen, X.Y. Wang, Y.Z. Li, Z.J. Guo. *Inorg. Chem. Commun.*, **11**, 1392 (2008).
[6] X. Sheng, X. Guo, X.M. Lu, G.Y. Lu, Y. Shao, F. Liu, Q. Xu. *Bioconjugate Chem.*, **19**, 490 (2008).

[7] P.U. Maheswari, S. Roy, H. den Dulk, S. Barends, G. van Wezel, B. Kozlevčar. *J. Am. Chem. Soc.*, **128**, 710 (2006).
[8] J. Chin, M. Banaszczyk, V. Jubian, X. Zou. *J. Am. Chem. Soc.*, **111**, 186 (1989).
[9] Z.L. Lu, C.T. Liu, A.A. Neverov, R.S. Brown. *J. Am. Chem. Soc.*, **129**, 11642 (2007).
[10] S. Anbu, M. Kandaswamy, P. Suthakaran, V. Murugan, B. Varghese. *J. Inorg. Biochem.*, **103**, 401 (2009).
[11] D.M. Kong, J. Wang, L.N. Zhu, Y.W. Jin, X.Z. Li, H.X. Shen, H.F. Mi. *J. Inorg. Biochem.*, **102**, 824 (2008).
[12] J. Liu, T.B. Lu, H. Li, Q.L. Zhang, L.N. Ji. *Transition Met. Chem.*, **27**, 686 (2002).
[13] C.Y. Zhou. Synthesis, characterization of the metal complexes involving polyamide compounds and their interaction with DNA. Doctoral diss., Shanxi University (2007).
[14] R.R. Gagne, C.L. Spiro, T.J. Smith, C.A. Hamann, W.R. Thies, A.K. Shiemke. *J. Am. Chem. Soc.*, **103**, 4081 (1981).
[15] G.P. Moloney, D.P. Kelly, P. Mack. *Molecules*, **6**, 234 (2001).
[16] Q.D. Zeng, M. Qian, S.H. Gou, H.K. Fun, C.Y. Duan, X.Z. You. *Inorg. Chim. Acta*, **294**, 2 (1999).
[17] SMART and SAINT. *Area Detector Control and Integration Software*, Siemens Analytical X-ray Systems Inc., Madison, WI, USA (1996).
[18] G.M. Sheldrick, *SHELXTL V5.1, Software Reference Manual*, Bruker AXS, Inc., Madison, WI, USA (1997).
[19] M.E. Reichmann, S.A. Rice, C.A. Thomas, P. Doty. *J. Am. Chem. Soc.*, **76**, 3047 (1954).
[20] A.M. Pyle, J.P. Rehmann, R. Meshoyrer, C.V. Kumar, N.J. Turro, J.K. Barton. *J. Am. Chem. Soc.*, **111**, 3055 (1989).
[21] J.K. Barton, A.T. Danishefsky, J.M. Goldberg. *J. Am. Chem. Soc.*, **106**, 2172 (1984).
[22] A. Neves, M.A. de Brito, I. Vencato, V. Drago, K. Griesar, W. Haase. *Inorg. Chem.*, **35**, 2360 (1996).
[23] B.P. Gaber, V. Miskowski, T.G. Spiro. *J. Am. Chem. Soc.*, **96**, 6868 (1974).
[24] P.S. Guin, P.C. Mandal, S. Das. *J. Coord. Chem.*, **65**, 705 (2012).
[25] A. Patra, S. Sen, S. Sarkar. *J. Coord. Chem.*, **65**, 4096 (2012).
[26] R. Prabu, A. Vijayaraj, R. Suresh. *J. Coord. Chem.*, **66**, 206 (2013).
[27] S.C. Zhang, J.J. Dong, X.R. Fan. *J. Coord. Chem.*, **66**, 3098 (2013).
[28] H.L. Wu, J.K. Yuan, Y. Bai. *J. Coord. Chem.*, **65**, 616 (2012).
[29] F. Zhang, Q.Y. Lin, W.D. Liu. *J. Coord. Chem.*, **66**, 2297 (2013).
[30] F.J. Meyer-Almes, D. Porschke. *Biochemistry*, **32**, 4246 (1993).
[31] J.B. LePecq, C. Paoletti. *J. Mol. Biol.*, **27**, 87 (1967).
[32] B. Li, W. Liu, J. Shao. *J. Coord. Chem.*, **66**, 2465 (2013).